

## Temperature and size dependence of time-resolved exciton recombination in ZnO quantum dots

I. Musa, F. Massuyeau, L. Cario, J. L. Duvail, S. Jobic et al.

Citation: *Appl. Phys. Lett.* **99**, 243107 (2011); doi: 10.1063/1.3669511

View online: <http://dx.doi.org/10.1063/1.3669511>

View Table of Contents: <http://apl.aip.org/resource/1/APPLAB/v99/i24>

Published by the [American Institute of Physics](http://www.aip.org).

---

### Additional information on *Appl. Phys. Lett.*

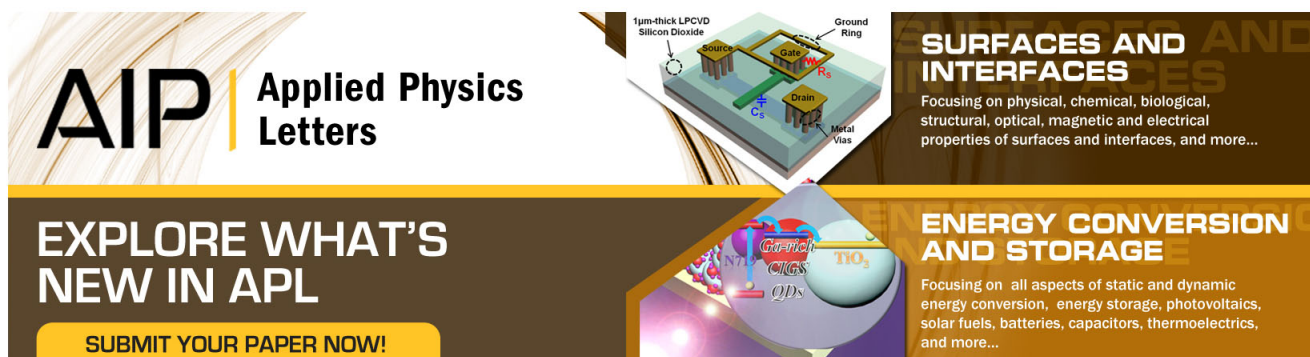
Journal Homepage: <http://apl.aip.org/>

Journal Information: [http://apl.aip.org/about/about\\_the\\_journal](http://apl.aip.org/about/about_the_journal)

Top downloads: [http://apl.aip.org/features/most\\_downloaded](http://apl.aip.org/features/most_downloaded)

Information for Authors: <http://apl.aip.org/authors>

## ADVERTISEMENT



**AIP** | Applied Physics  
Letters

**EXPLORE WHAT'S  
NEW IN APL**

**SUBMIT YOUR PAPER NOW!**

**SURFACES AND INTERFACES**  
Focusing on physical, chemical, biological, structural, optical, magnetic and electrical properties of surfaces and interfaces, and more...

**ENERGY CONVERSION AND STORAGE**  
Focusing on all aspects of static and dynamic energy conversion, energy storage, photovoltaics, solar fuels, batteries, capacitors, thermoelectrics, and more...

Labels in the 3D schematic: 1µm-thick LPCVD Silicon Dioxide, Source, Gate, Drain, Metal Vias, Ground Ring, Cs, R<sub>s</sub>.

Labels in the energy conversion diagram: QDs, NTG, CIGS, NO<sub>2</sub>.

# Temperature and size dependence of time-resolved exciton recombination in ZnO quantum dots

I. Musa,<sup>1</sup> F. Massuyeau,<sup>1</sup> L. Cario,<sup>1</sup> J. L. Duvail,<sup>1</sup> S. Jobic,<sup>1</sup> P. Deniard,<sup>1</sup> and E. Faulques<sup>1,2,a)</sup>

<sup>1</sup>Institut des Matériaux Jean Rouxel, Université de Nantes, CNRS, UMR6502, 2 rue de la Houssinière, 44322 Nantes, France

<sup>2</sup>Department of Physics, University of Warwick, Gibbet Hill Road, Coventry CV4 7AL, United Kingdom

(Received 22 October 2011; accepted 21 November 2011; published online 14 December 2011)

ZnO nanocrystals with various sizes were prepared and characterized. Their photoluminescence dynamics has been investigated at low temperatures. For the smallest particles (3 nm), a defect-induced long-lived photoluminescence occurs around 2.5 eV which is slowed down at decay times longer than 3 ns when sample temperature  $T$  decreases. From thermal quenching of the 2.5 eV band, the exciton dissociation energy at defect centers is estimated around  $\sim 11.8$  meV. For larger crystallites (10 and 20 nm), the ultraviolet emission observed at 3.32 eV decays in less than 85 ps and follows a Varshni law [Y. P. Varshni, *Physica (Amsterdam)* **34**, 149 (1967)]. © 2011 American Institute of Physics. [doi:10.1063/1.3669511]

ZnO is a wide bandgap n-type semiconductor suitable for devices and ultraviolet (UV) lasers,<sup>1–3</sup> which exhibits two strong photoluminescence (PL) masses in the UV and visible range at room temperature (RT).<sup>4</sup> The first UV emission at 3.30 eV (375 nm) is usually ascribed to the main contribution of near-band-edge (NBE) free excitons. The broader ZnO emission of the green spectral range (hereafter referred to as G band) occurs between 2.2–2.5 eV (480–560 nm) and reflects various types of intrinsic defects always present in the ZnO structure, especially occurring in quantum dots (QDs) and nanocrystals.<sup>5</sup>

While absorption and fluorescence studies of ZnO QDs are well documented, there are fewer reports<sup>6,7</sup> on the combined influence of sample temperature, size, and intrinsic defects on the quantum confinement effect and the exciton decay dynamics of both NBE and G bands in ZnO nanostructures. In this letter, we study these properties on as-synthesized pristine ZnO nanocrystals with different controlled sizes (3–20 nm) produced by soft chemistry routes.<sup>8,9</sup> Transmission electron microscopy (TEM) images and x-ray diffraction Rietveld refinements show that our ZnO nanoparticle syntheses give apparent sizes of 3, 5, 10, 20 nm, and 4.5, 5, 10.5, 24.2 nm, respectively. The nanoparticles have a characteristic hexagonal shape with the wurtzite structure type.

We expect that our smallest nanoparticles of size 3 nm with a radius smaller than the bulk ZnO Bohr radius ( $a_B = 2.34$  nm) (Ref. 10) can have relatively high exciton energy, and that charge carriers are in the strong confinement regime. Exciton energy in quantum dots with radius larger than the ZnO Bohr radius is relatively smaller in comparison, and carriers in these dots are in the weak quantum confinement regime. Thus, in the present work, our ZnO nanoparticles of size 5 nm and size 10–20 nm should lie in the intermediate and weak confinement regimes, respectively.

Fig. 1(a) shows that the optical absorption edge depicting the energy of the lowest excited state of the exciton shifts towards high energies as the size of our particles decreases. This trend can be reproduced by expressing the energy of the lowest excited state as a function of the nanocrystal radius  $R$ ,<sup>11</sup>

$$E(R) = E_g + \frac{\hbar^2 \pi^2}{2R^2 \mu} - \frac{1.786e^2}{4\pi\epsilon_0\epsilon R}, \quad (1)$$

where  $\epsilon_0$  and  $\epsilon$  are the permittivities of free space and particles,  $e$  the elementary charge, and  $\mu$  the reduced effective mass of the electron ( $m_e^*$ ) and the hole ( $m_h^*$ ). The best fit with Eq. (1) to the experimental absorption mid-edge energies is obtained for  $m_e^* = 0.24$ ,  $m_h^* = 0.45$ , and  $\epsilon = 3.7$  in good agreement with an intermediate confinement regime

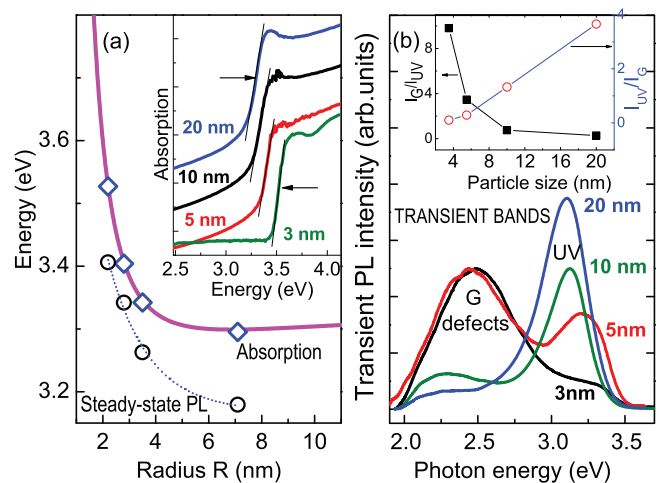


FIG. 1. (Color online) (a) Optical absorption and steady-state PL at RT of ZnO nanocrystals of various average diameters: dependence of the lowest excited state and PL maximum vs. radii. Diamonds and circles correspond to the optical absorption edges (arrows) and PL maxima (excitation,  $\lambda_{exc} = 325$  nm), respectively. (b) Time-resolved PL spectra (RT,  $\lambda_{exc} = 267$  nm) for ZnO nanoparticles, over 1 ns. Inset: Variation of the transient PL intensity ratio of G and UV bands against size.

<sup>a)</sup> Author to whom correspondence should be addressed. Electronic mail: eric.faulques@cnrs-imn.fr.

characterized by  $m_e^* < m_h^*$ .<sup>12</sup> This curve yields averaged particle sizes in solution of 4, 6, 7, and 14 nm. It is seen that  $E$  is almost saturated while extending to the upper size limit.<sup>13</sup> The particles were studied additionally using steady-state PL with resonant excitation at 325 nm (3.81 eV). A strong UV peak is observed, progressively red-shifted as size increases (Fig. 1(a), lower curve), and located at 3.406, 3.342, 3.263, and 3.179 eV for 3, 5, 10, and 20 nm diameters, respectively. This PL band has been resolved into several constituent bands stemming from acceptor-bound AX excitons, donor-bound DX excitons (at 3.25 eV), and free X excitons.<sup>6,7,14</sup> The confinement effect is confirmed by a Stokes-shift increase of about 100 meV from 20-nm to 3-nm size.<sup>12,14,15</sup>

To see the influence of size, defects, and low temperatures on the excitonic dynamics, we have performed time resolved PL experiments using a femtosecond laser and a streak camera system as in our previous studies.<sup>16,17</sup> Fig. 1(b) shows the room-temperature transient PL spectra, integrated over a time of 1 ns, for the different sizes. All nanoparticles show two distinct transient emission bands, the UV peak matching well the resonantly excited ZnO near-band-edge steady-state emission around 3.10–3.3 eV with a minor unresolved band around 2.98 eV, and a broad emission G-band in the blue-green region of the spectrum which is attributed, like for the steady-state PL case, to intrinsic point defects.<sup>18</sup> There is also a blue shift of the transient UV peak from 3.10 to 3.35 eV ( $\Delta E = 0.25$  eV) with size reduction. Results of Figs. 1(a) and 1(b) can be naturally explained by the quantum confinement, which shifts the energy levels of the conduction and valence bands apart, causing a blue shift in the transition energy as the size of nanoparticles decreases.

An intriguing result here is that the relative intensity of the two transient PL bands depends on the size of the nanoparticles. The inset of Fig. 1(b) shows that the defect-related transient band peaked around 2.5 eV (G band) is strongly enhanced with size reduction, i.e., with the increase of the total surface area in the particle ensemble volume resulting from the larger surface area to volume ratio.<sup>19</sup> Between the two extreme sizes, this intensity enhancement is roughly of a factor of 10. Additionally, we observe that the emission of the defect-induced G band is longer-lived as the size of nanoparticles decreases at RT (Fig. 2(a), inset). These data sug-

gest that several trap states originating from surface defects are involved in the radiative recombination occurring around 2.5 eV in smaller particles. The luminescent species trapped at surface defects survive longer before recombination without being perturbed by their environment. In this case, the luminescence decay is longer-lived. From the energy difference at stake ( $>3k_B T$ ), we may ascribe the 2.5 eV emission (2.6 eV at 10 K) to a transition involving nonbonding donor oxygen-vacancy levels formed from  $sp^3$  hybrid orbitals and located in the gap.<sup>5,20</sup>

Temperature dependent experiments down to  $T = 8$ –15 K were carried out for all samples. For the smaller 3-nm QDs (Fig. 2(a)), we record the strong defect band around 2.57 eV with a small low energy component at 2.17 eV. The PL kinetics (Fig. 2(b)) are reproduced by a Kohlrausch-Williams-Watts law,<sup>21</sup>

$$n(t) = n_0 \exp[-(t/\tau_k)^{\beta_k}]. \quad (2)$$

Here,  $n_0$  is the exciton population  $n(t=0)$  and  $\tau_k$  the characteristic Kohlrausch time. The stretching exponent ( $0 < \beta_k \leq 1$ ) can be expressed by  $\beta_k = D/(D+2)$ , where  $D$  is the effective dimensionality of the configuration space in which the excitons relax.<sup>22</sup> The average lifetime of this distribution is  $\langle \tau \rangle = \tau_k \beta_k^{-1} \Gamma(\beta_k^{-1})$ , where  $\Gamma$  is the Gamma function. Assignment of Eq. (2) to experimental decays of ZnO nanocrystals is justified in the case of ensembles in which particles are not isolated from each other. The average decay time of the 3-nm QD defect emission is strongly  $T$ -dependent raising from 1888 ps at RT to 3194 ps at 10 K with drastic increase below 150 K. Concomitantly, the dimensional parameter  $\beta_k$  decreases from 0.69 at RT to 0.58 at 10 K; i.e., the PL relaxation is more dispersive with more spread relaxation rates. In this case, there is slower 3D relaxation in the presence of short range forces. We measure a small upshift in energy of 30 meV between ambient temperature and 10 K.

The thermal quenching of the G band can be directly obtained from the decay curves of Fig. 2(b). The plot of the PL intensity 4 ns after excitation vs.  $1/T$  can be reproduced by an Arrhenius model,<sup>23</sup>

$$I_{PL}(T) = I_0 [1 + c_1 \exp(-E_1/k_B T) + c_2 \exp(-E_2/k_B T)]^{-1}, \quad (3)$$

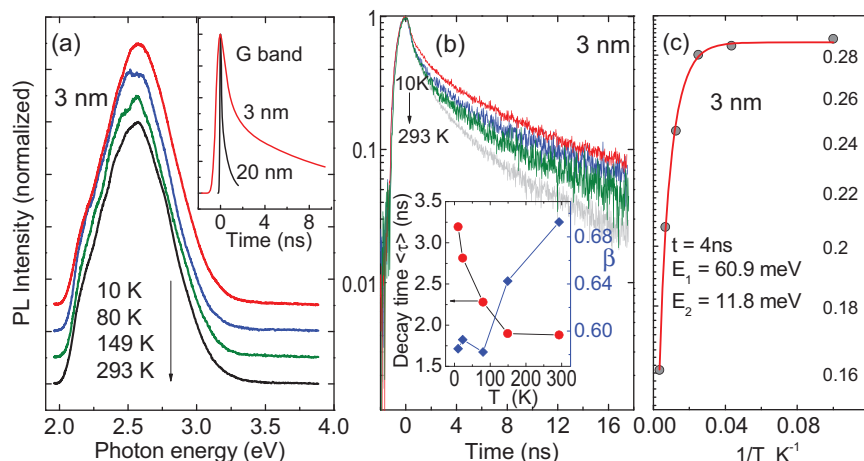


FIG. 2. (Color online) Temperature dependence of the transient PL for 3-nm ZnO nanoparticles from RT to 10 K. Time-resolved emission spectra (a). In inset, the decays of the G band for the two extreme sizes 3 nm ( $\langle \tau \rangle = 1.88$  ns,  $\beta_k = 0.69$ ) and 20 nm ( $\langle \tau \rangle = 309$  ps,  $\beta_k = 0.71$ ) are compared at RT. PL kinetics of 3 nm nanocrystals (b) with signals spectrally integrated between 1.96 eV and 3.87 eV. Inset: Variation of the average Kohlrausch lifetime and stretching exponent from fits to the decays. Thermally activated PL quenching of the G band at  $t = 4$  ns after excitation (c);  $\lambda_{exc} = 267$  nm.



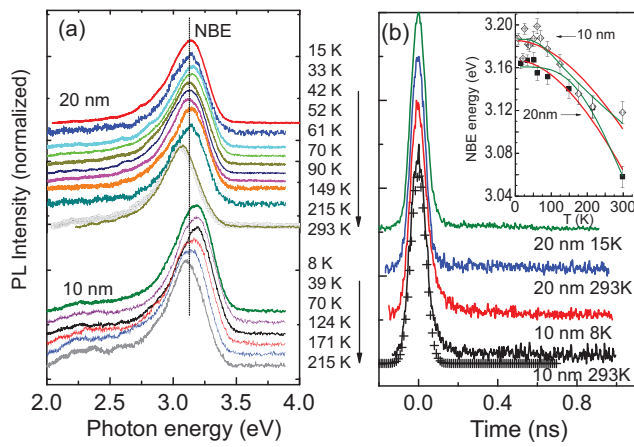


FIG. 3. (Color online) Temperature dependence of the transient PL of ZnO nanoparticles from RT to 8 K. Time-resolved emission spectra of the NBE exciton versus  $T$  for 10-nm and 20-nm ZnO QDs (a); corresponding temporal signals close to the apparatus function (crosses) (b) with lifetimes  $< 85$  ps. Inset: Energies of NBE emission as function of  $T$  for 10-nm and 20-nm ZnO nanocrystals fitted by Varshni laws in " $T^2$ " (thick lines, Debye temperature  $\theta_D = 920$  K) and in " $T^4$ " (thin lines);  $\lambda_{exc} = 267$  nm.

where  $I_0$  is the peak intensity at  $T = 0$  K,  $c_1$ ,  $c_2$  parameters, and  $k_B$  is the Boltzmann constant. The fit to the data yields  $E_1 = 60.9 \pm 10.5$  meV, close to the free exciton binding energy in bulk ZnO, and  $E_2 = 11.8 \pm 1.2$  meV corresponding to the dissociation energy of the excitons trapped at defects (Fig. 2(c)). Then it is likely that the 3-nm QD emission is dominated by recombination at defects with a minor contribution from the NBE excitonic part (see Fig. 1(b), black line) with activation energy of about 60 meV.

In the case of 10-nm and 20-nm QDs (Fig. 3), the NBE exciton emission is redshifted and the PL intensity is also thermally quenched as temperature increases. The maximum of the PL emission in these samples conforms well to a Varshni law,<sup>24</sup>

$$E_{PL}(T) = E_0 - \frac{\alpha T^2}{\beta + T}, \quad (4)$$

with  $E_0 = 3.167$  eV (20 nm) and 3.185 eV (10 nm) being the transition energies at 0 K,  $\alpha = 14 \times 10^{-4}$  (20 nm) and  $11.3 \times 10^{-4}$  eV K<sup>-1</sup> (10 nm), and  $\beta = 920$  K (Fig. 3(b)). We could also obtain a better fit of the data at low  $T$  with a modified Varshni law where  $\alpha T^2 \rightarrow \alpha T^4$  and  $\beta + T \rightarrow \beta + T^3$ .<sup>25</sup> The difference between the fits and the experimental points is less than 3 meV below 14 K which is typical of free excitons rather than localized excitons.<sup>7</sup> The lifetime of these NBE excitons is too short ( $< 85$  ps) to observe a temporal dependence with temperature.

In summary, we have reported temperature dependent time-resolved PL experiments on ZnO QDs with different sizes. We have demonstrated the different exciton kinetics of

the two major emissions related to confined excitons in the UV region and to defects in the green spectral range. The former ultrashort-lived UV band shifts to higher energy when QD size is augmented. This emission follows a Varshni law at low temperatures showing that it originates mainly from free excitons. The latter PL band tentatively ascribed to oxygen vacancies at dot surfaces shows long-lived decays with exciton dissociation energy of about 11.8 meV.

This work was partly supported by the French-Ukrainian Contract PICS No. 4766 between NASU and CNRS.

- <sup>1</sup>M. H. Huang, S. Mao, H. Feick, H. Yan, Y. Wu, H. Kind, E. Weber, R. Russo, and P. Yang, *Science* **292**, 1897 (2001).
- <sup>2</sup>J. S. Bendall, G. Visimberga, M. Szachowicz, N. O. V. Plank, S. Romanov, C. M. Sotomayor-Torres, and M. E. Welland, *J. Mater. Chem.* **18**, 5259 (2008).
- <sup>3</sup>K. Borgohain and S. Mahamuni, *Semicond. Sci. Technol.* **13**, 1154 (2008).
- <sup>4</sup>D. Bera, L. Qian, S. Sabui, S. Santra, and P.-H. Holloway, *Opt. Mater.* **30**, 1233 (2008).
- <sup>5</sup>A. Janotti and C. G. Van de Walle, *Rep. Prog. Phys.* **72**, 126501 (2009).
- <sup>6</sup>V. A. Fonoberov, K. A. Alim, A. A. Balandin, F. Xiu, and J. Liu, *Phys. Rev. B* **73**, 165317 (2006).
- <sup>7</sup>L. Béaur, T. Bretagnon, B. Gil, A. Kavokin, T. Guillet, C. Brimont, D. Tainoff, M. Teisseire, and J.-M. Chauveau, *Phys. Rev. B* **84**, 165312 (2011).
- <sup>8</sup>V. Noack and A. Eychmüller, *Chem. Mater.* **14**, 1411 (2002).
- <sup>9</sup>N. Uekawa, N. Mochizuki, J. Kajiwara, F. Mori, Y. J. Wu, and K. Kakegawa, *Phys. Chem. Chem. Phys.* **5**, 929 (2003).
- <sup>10</sup>R. T. Senger and K. K. Bajaj, *Phys. Rev. B* **68**, 045313 (2003).
- <sup>11</sup>L. E. J. Brus, *Chem. Phys.* **80**, 4403 (1984).
- <sup>12</sup>K.-F. Lin, H.-M. Cheng, H.-C. Hsu, L.-J. Lin, and W. F. Hsieh, *Chem. Phys. Lett.* **409**, 208 (2005).
- <sup>13</sup>J. C. Nie, J. Y. Yang, Y. Piao, H. Li, Y. Sun, Q. M. Xue, C. M. Xiong, R. F. Dou, and Q. Y. Tu, *Appl. Phys. Lett.* **93**, 173104 (2008).
- <sup>14</sup>G. Kiliani, R. Schneider, D. Litvinov, D. Gerthsen, M. Fonin, U. Rüdiger, A. Leitenstorfer, and R. Bratschitsch, *Opt. Express* **19**, 1641 (2011).
- <sup>15</sup>In this work, we define the Stokes shift as the energy difference between the absorption maximum (different from the absorption edge energy) and the maximum of the steady-state photoluminescence peak in the UV range.
- <sup>16</sup>E. Faulques, V. G. Ivanov, G. Jonusauskas, H. Athalin, O. Pyshkin, J. Wéry, F. Massuyeau, and S. Lefrant, *Phys. Rev. B* **74**, 075202 (2006).
- <sup>17</sup>E. Faulques, F. Massuyeau, Q. Wang, D.-K. Seo, and S. Jobic, *Appl. Phys. Lett.* **97**, 153111 (2010).
- <sup>18</sup>M. D. McCluskey and S. J. Jokela, *J. Appl. Phys.* **106**, 071101 (2009).
- <sup>19</sup>K. Suzuki, H. Kondo, M. Inoguchi, N. Tanaka, K. Kageyama, and H. Takagi, *Appl. Phys. Lett.* **94**, 223103 (2009).
- <sup>20</sup>D. M. Hoffmann, D. Pfisterer, J. Sann, B. K. Meyer, R. Tena-Zaera, V. Munoz-Sanjose, T. Frank, and G. Pensl, *Appl. Phys. A* **88**, 147 (2007).
- <sup>21</sup>G. Beadie, E. Sauvain, A. S. L. Gomes, and N. M. Lawandy, *Phys. Rev. B* **51**, 2180 (1995).
- <sup>22</sup>J. C. Phillips, *Phys. Rev. B* **52**, R8337 (1995).
- <sup>23</sup>M. Leroux, N. Grandjean, B. Beaumont, G. Nataf, F. Semond, J. Massies, and P. Gibart, *J. Appl. Phys.* **86**, 3721 (1999).
- <sup>24</sup>Y. P. Varshni, *Physica (Amsterdam)* **34**, 149 (1967).
- <sup>25</sup>M. Cardona, T. A. Meyer, and M. L. W. Thewalt, *Phys. Rev. Lett.* **92**, 196403 (2004).